SCIENTIFIC REPORTS

OPEN

SUBJECT AREAS:
ELECTRONIC DEVICES
SOLAR CELLS
NANOPARTICLES
SYNTHESIS AND PROCESSING

Received
26 November 2012

Accepted
4 March 2013

Published
20 March 2013

Correspondence and requests for materials should be addressed to C.-W.H. (hanchi@kier.re.kr) or S.-G.Y. (sgyoon@cnu.ac.kr)

Formation of artificial pores in nano-TiO_2 photo-electrode films using acetylene-black for high-efficiency, dye-sensitized solar cells

Tae-Yeon Cho[1], Chi-Whan Han[2], Yongseok Jun[3] & Soon-Gil Yoon[4]

[1]Sollar Cell R&D Team, SeAH E&T Co. 1688-1, Shinil-Dong, Daeduk-Gu, 306-230, Daejeon, Korea, [2]Photovoltaic Research Center, Korea Institute of Energy Research, 305-343, Daejeon, Korea, [3]Interdisciplinary School of Green Energy, Ulsan National Institute of Science and Technology, UNIST-gil 50, 689-798, Ulsan, Korea, [4]Department of Materials Engineering, Chungnam National University, Daeduk Science Town, 305-764, Daejeon, Korea.

Acetylene-black paste without a light scattering layer was applied to meso-porous TiO_2 photo-electrode films with a crystalline framework, a low residual carbon, and a tunable morphological pore size. The thermal-treated TiO_2 photo-electrode films had an increased acetylene-black concentration with an increase in artificial pores and a decrease in residual carbon. The performance of dye-sensitized solar cells (DSSCs) was enhanced by the use of the TiO_2 photo-anode pastes at various acetylene-black concentrations. The photo-conversion efficiency of the DSSCs using TiO_2 photo-electrode films with 1.5 wt% acetylene-black was enhanced from 7.98 (no acetylene-black) to 9.75% without the integration of a light- scattering layer.

Dye-sensitized solar cells (DSSC) are photoelectric chemical solar cells with a ca. 38% theoretical maximum value for photoelectric conversion efficiency and a relatively low fabrication cost[1–3]. The maximum photoelectric conversion efficiency of DSSCs recently achieved in a laboratory was already more than 11%[4–6]. The typical working electrode for a DSSC is generally composed of a dye attached to meso-porous TiO_2 films coated onto a transparent conductive oxide (TCO)/glass substrate[7,8]. A platinized conductive glass is used as a counter electrode and an electrolyte containing an I^-/I_3^- redox couple is used to fill in between the two electrodes. The performance of DSSCs depends on a combination of various factors, such as the morphology and structure of the TiO_2 photo-electrode, dye molecules[4], the electrolyte[9,10], the platinum counter electrode[11], and the transparent conductive oxide (TCO) layer.

Recent improvements have been reported in the light harvest efficiency of a dye-adsorbed TiO_2 electrode via light scattering[12–15]. The light-scattering effect was achieved by the addition of TiO_2 layers. The addition of scattering layers with the TiO_2 large particles ensures adequate light trapping in the device[16,17], due to an increase in the absorption path length of photons and optical confinement. Ferber et al.[18] and Rothenberger et al.[19] confirmed the light-scattering effect using the transport theory and a many-flux model, respectively. Given the scattering abilities of TiO_2 films, it is also important that the TiO_2 electrode have a high surface area, which is responsible for optimal dye loading and effective photocurrent generation. However, to date, a high photo-conversion efficiency for DSSCs has not been reported without the use of a light-scattering layer.

In the present study, the TiO_2 photo-electrode films with artificial pores formed using acetylene-black were prepared to improve the light harvest efficiency of DSSCs without a light scattering layer. The structural and the photovoltaic properties of the DSSCs were compared with TiO_2 photo-electrode films without (hereafter referred to as the Normal films) and with different acetylene-black concentrations. The acetylene-black was introduced for a light-scattering role and morphology change of the electrode and for a reduction of residual carbons in the TiO_2 photo-electrode films.

Results

Thermal properties of the acetylene-black were characterized using Thermogravimetric/Differential Thermal Analysis (TG/DTA) technique. Figure 1(a) shows the TG/DTA results of the TiO_2 photo-anode paste including 1.5 wt% acetylene-black. The TG/DTA results were recorded from 30 to 900°C at a heating rate of 5°C/min. An

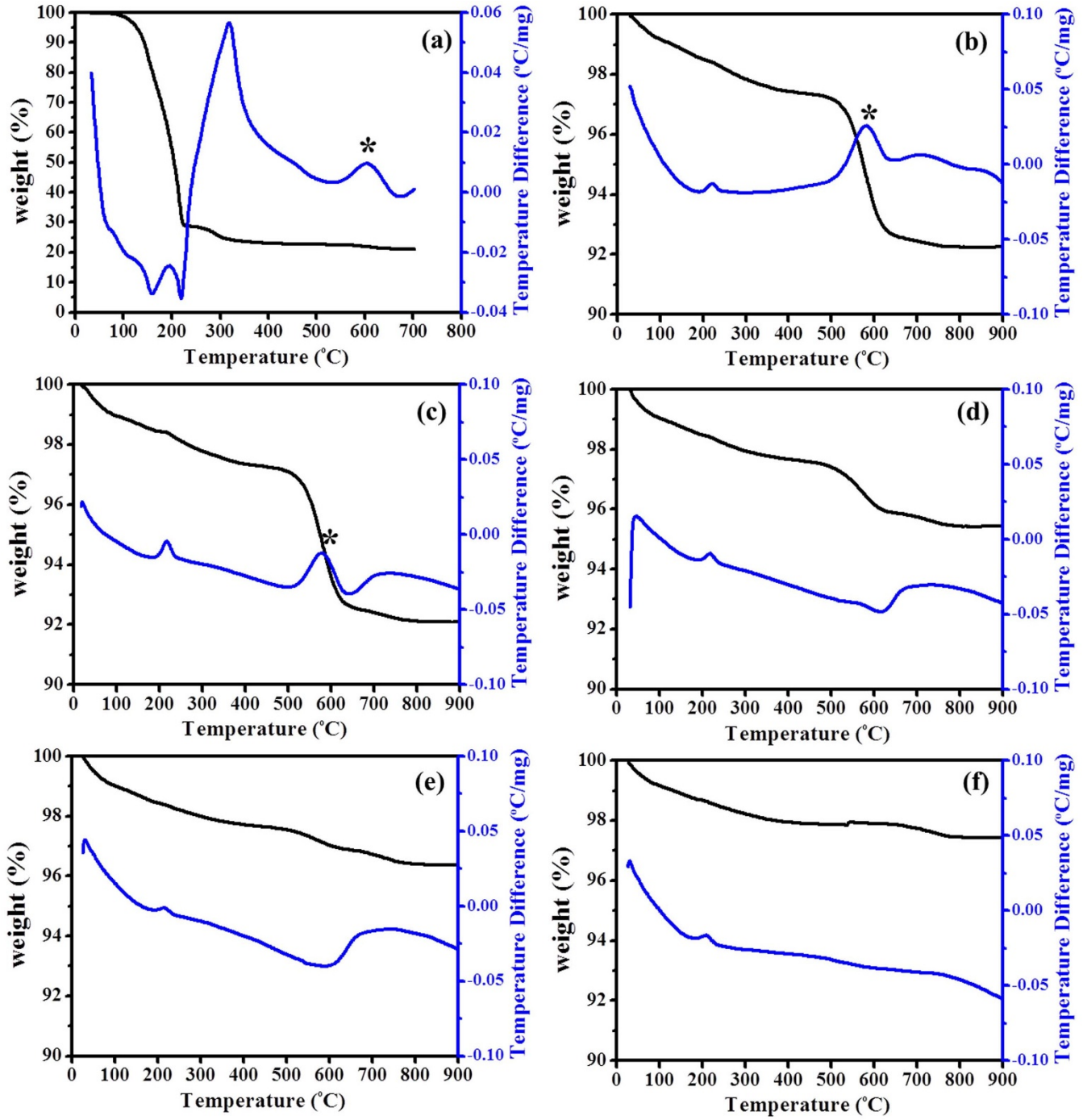

Figure 1 | TG/DTA plots recorded from 30 to 900°C at a heating rate of 5°C/min using the TiO_2 photo-anode paste including (a) 1.5 wt% acetylene-black. TG/DTA plots recorded from 30 to 900°C at a heating rate of 5°C/min using 1.5 wt% acetylene-black TiO_2 paste samples treated at (b) 350, (c) 400, (d) 450, (e) 500, and (f) 550°C for 30 min. The "asterisk" in the figures means the exothermic peak which exhibited the thermal decomposition of acetylene-black.

endothermic peak was observed at 159°C and three exothermic peaks were observed at 194, 319 and 604°C. The endothermic peak at 159°C was attributed to the evaporation of the remaining solvent. The first two exothermic peaks at 194 and 319°C may be attributed to the decomposition of the organic materials. The peaks at 604°C were attributed to the decomposition of the acetylene-black. The TG/DTA indicated that complete decomposition of acetylene-black occurred at 604°C, which resulted in a temperature that was too high for the FTO/glass process. However, DSSC devices using TiO_2 photo-anode pastes with acetylene-black actually were thermally treated at 500°C for 30 min in the present study. In order to decide the real decomposition temperature of the acetylene-black for DSSC cells, TiO_2 photo-anode pastes, including 1.5 wt% acetylene-black, were thermally treated at 350, 400, 450, 500, and 550°C for 30 min, and then samples treated at each temperature were measured at a heating rate of 5°C/min using TG/DTA. The results are shown in Figs. 1(b) ~ 1(f). Samples treated at 350 (Fig. 1(b)) and 400°C (Fig. 1 (c)) for 30 min showed peaks exhibiting a decomposition of acetylene-black at about 600°C. This result suggested that the acetylene-black still remained in the TiO_2-photo anode films treated at 350 and 400°C for

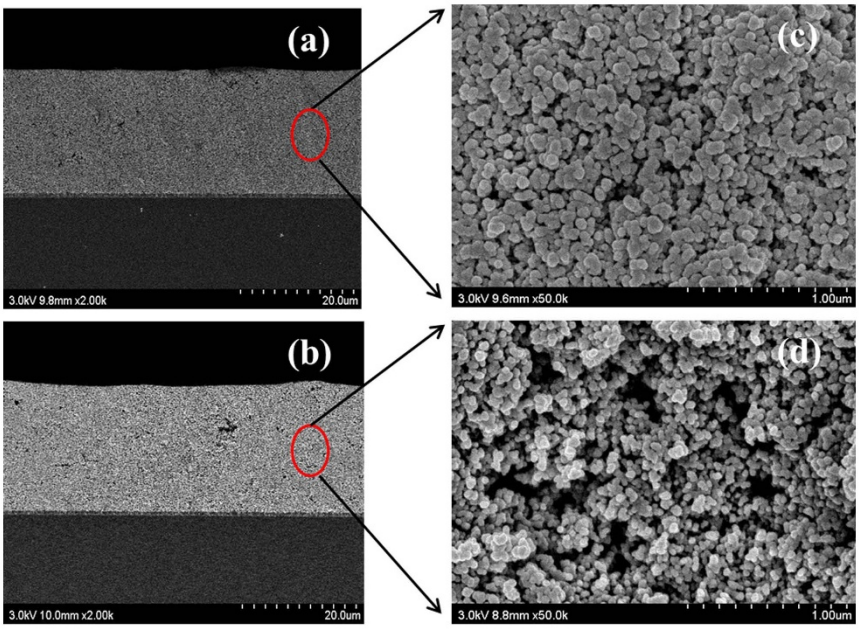

Figure 2 | SEM cross-sectional images of the TiO_2 photo-electrode films with acetylene-black of (a) 0 and (b) 1.5 wt%. (c), (d) Enlarged SEM image from the cross-section (red circle) of TiO_2 photo-electrode films with an acetylene-black of 0 and 1.5 wt%, respectively.

30 min. On the other hand, samples treated at 450°C (see Fig. 1(d)) showed no peak, which indicated the decomposition of acetylene-black, and resulted in a complete decomposition of the acetylene-black in samples treated at 450°C for 30 min. That result suggested that the DSSC cells composed of TiO_2 photo-electrode films treated at 500°C for 30 min showed a complete removal of the acetylene-black inserted in order to form the artificial pores in the TiO_2 films. In the same manner, for samples treated at 500 (Fig. 1(e)) and 550°C (Fig. 1(f)) for 30 min, we observed no DTA peaks indicating a decomposition of the acetylene-black. According to these results, the acetylene-black was completely removed from the DSSCs by thermal treatment at 450°C for 30 min.

Discussion

Figure 2 shows the scanning electron microscope (SEM) cross-sectional and surface images of the Normal films and TiO_2 photo-anode film with 1.5 wt% acetylene-black. The images of the TiO_2 photo-anodes were analyzed after a thermal treatment at 500°C for 30 min in air ambient. Cross-sectional image of the Normal films and TiO_2 photo-anode film with 1.5 wt% acetylene-black is shown in Fig. 2(a) and 2(b), respectively. The circled part in the cross-section of the Normal films and TiO_2 photo-anode film with 1.5 wt% acetylene black is enlarged to observe the grains and the pores clearly and it is shown in Fig. 2(c) and 2(d), respectively. As shown in the surface and cross-sectional images, the size of the pores is apparently increased by an insertion of acetylene-black, compared with that of the Normal films.

The Brunauer–Emmett–Teller (BET) method was used for observation of the surface area, average pore size, and the total pore volume of both the Normal films and the acetylene-black TiO_2 photo-electrode films. The results are summarized in Table 1. The specific surface area ($a_{s,BET}$) of the Normal photo-electrode film was 42.364 $m^2\ g^{-1}$ and that of the sample with 1.5 wt% acetylene-black was 36.382 $m^2\ g^{-1}$. Total pore volume of the Normal photo-electrode film was 0.186 $cm^3\ g^{-1}$ and that of the sample was 0.212 $cm^3\ g^{-1}$. The average pore size of the Normal film was 18 nm and that of the sample was 23 nm. The results show that the Normal films exhibited a comparatively smaller pore size than that of acetylene-black TiO_2 films and that acetylene-black TiO_2 films enhanced the light reflection capacities of the TiO_2 photo-electrode films. Generally, light is reflected through TiO_2 films when it irradiates into the photo-electrode. If the photo-electrode has strong scattering ability, much more light intensity is reflected back to the inner TiO_2 photo-electrode, which enhances the amount of light absorbed by the dye. The diffused reflectance spectra of the Normal films and 1.5 wt% acetylene-black TiO_2 photo-electrode films were measured using a spectrophotometer and are shown in Fig. 3(a). The diffused reflectance spectra were measured through the overall thickness of the TiO_2 photo-electrode films rather than the surface of the TiO_2 photo-electrode films. The acetylene-black TiO_2 photo-electrode films exhibited reflection capacities that were approximately 20% higher the Normal films in wavelengths that ranged between 400 and 800 nm. The results indicate that an incident light is reflected several times by the artificial pores in an acetylene-black TiO_2 photo-anode film, which further reinforces the light-harvesting ability of TiO_2, particularly in the visible range. Thus, artificial pores extend the photo-response into visible spectrum ranges, resulting in an enhancement of light utilization efficiency. Therefore, the slightly higher J_{SC} (Table 2) for acetylene-black TiO_2 photo-electrode films compared to the Normal films is a consequence of better light scattering.

The adsorption of the dye-molecules in the Normal films and TiO_2 films with different acetylene-black concentrations is compared in the UV-vis absorption spectra shown in Fig. 3(b). The results clearly indicate that the absorption by adsorbed dyes on the TiO_2 films with different acetylene-black concentrations is larger than the films with the same thickness as the Normal films. Especially, the absorbance of the Normal films abruptly decreased above a wavelength of 550 nm.

Table 1 | Average pore size, specific surface area, and total pore volume of the Normal films and the TiO_2 photo-electrode films with different acetylene-black concentrations

TiO_2 photo-electrode films	Normal	0.5 wt%	1.5 wt%	2.0 wt%
Average Pore Size (nm)	17.572	21.750	23.298	23.665
$a_{s,BET}$ (m^2g^{-1})	42.364	39.352	36.382	33.089
Total pore volume(cm^3g^{-1})	0.186	0.196	0.212	0.196

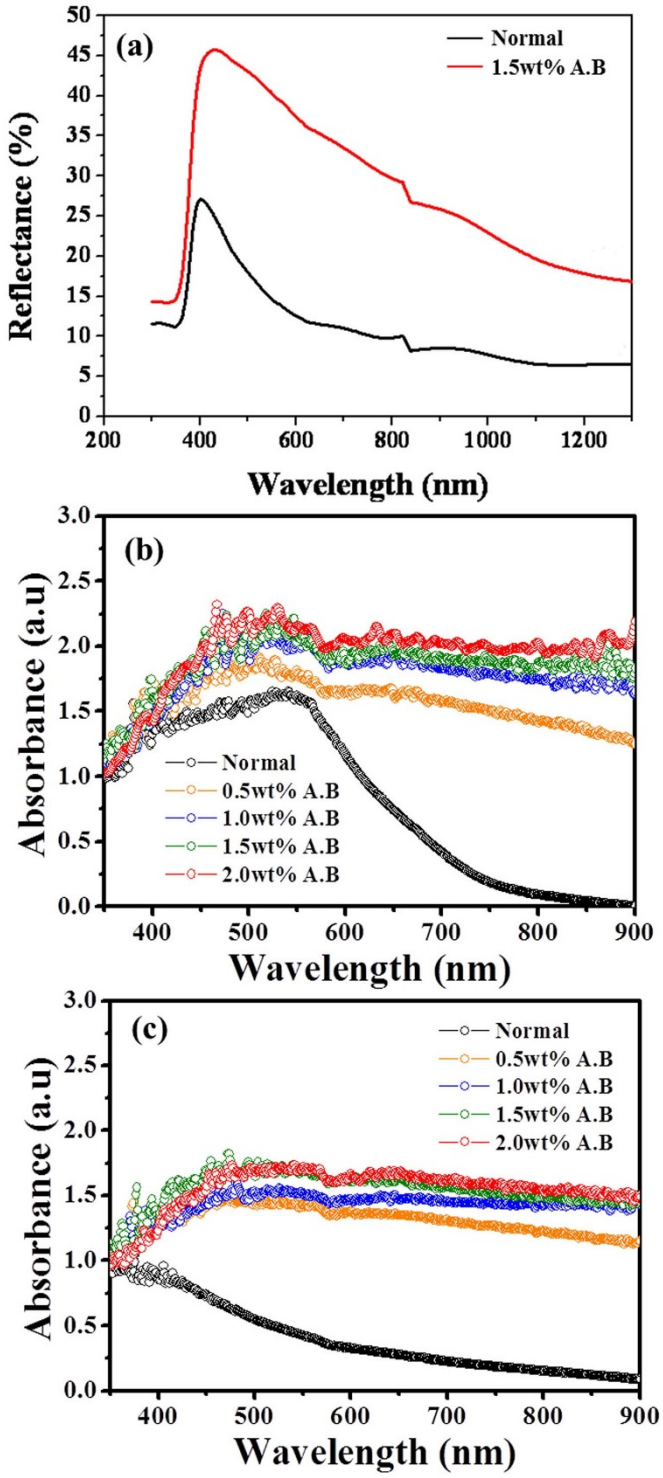

Figure 3 | (a) Reflectance vs. wavelength of the Normal films and the TiO_2 photo-electrode films with 1.5 wt% acetylene-black. (b), (c) Absorbance vs. wavelength of the Normal films and the TiO_2 photo-electrode films with different acetylene-black concentrations with and without dye, respectively. Here, A.B. denotes the acetylene-black.

On the other hand, those of the TiO_2 films with different acetylene-black concentrations were slightly decreased as wavelength increased above 550 nm. Absorbance results of the Normal films and the TiO_2 photo-electrode films with different acetylene-black concentrations without a dye-adsorption are shown in Fig. 3(c). An abrupt decrease in the absorbance with an increase in the wavelength in the Normal films was attributed to an increase in transmittance by a small quantity of pores. On the other hand, an increase in pores in the TiO_2 photo-electrode films with different acetylene-black concentrations increased the absorbance of the light in wavelengths that ranged from 350 to 900 nm. The quantitative amount of the adsorbed dye molecules in the Normal films and TiO_2 films with 1.5 wt% acetylene-black was approximately 0.03425 and 0.03869 mmol g^{-1}, respectively. Although the specific surface area of the Normal films is larger than that of the 1.5 wt% acetylene-black TiO_2 photo-electrode films, an increase of the adsorbed dye molecules in the TiO_2 films including the acetylene-black was attributed to the less carbon contaminations by a removal of the acetylene-black. The residual carbon concentrations in the Normal and acetylene-black TiO_2 films were shown in the later discussion. Lee et al. reported that the more dyes were adsorbed on the TiO_2 surface having less carbon contaminations by the UV-O_3 treatment[20]. The present results were consistent with those of the TiO_2 films treated with UV-O_3 process. In the result, the less carbon contaminations of TiO_2 surface having the artificial pores created by a removal of the acetylene-black increased the amount of the adsorbed dye-molecules, compared with the Normal films.

Table 2 | Photovoltaic parameters of the DSSCs fabricated using TiO_2 photo-electrode films prepared without (the Normal films) and with different acetylene-black concentrations

Acetylene-black (wt%)	J_{sc} (mA/cm^2)	V_{oc} (V)	FF	Efficiency(η) (%)
Normal	14.75	0.79	0.68	7.98
0.5	17.73	0.79	0.64	8.99
1.0	17.86	0.80	0.65	9.26
1.5	18.54	0.80	0.66	9.75
2.0	17.32	0.78	0.63	8.51
3.0	16.69	0.77	0.63	8.16

The Normal films and five different acetylene-black TiO_2 photo-electrodes were investigated for photo-conversion efficiency of DSSCs. The five different acetylene-blacks varied from 0.5, 1.0, 1.5, 2.0, and 3.0 wt%. Figure 4 shows the photo-current vs. voltage (*I–V*) curves of the DSSCs as a function of the acetylene-black concentration. The photovoltaic parameters of the DSSCs prepared with different acetylene-black concentrations are summarized in Table 2. Compared with the Normal films DSSC, photovoltaic parameters such as short-circuit current density (J_s) and open-circuit voltage (V_{oc}) were enhanced with increasing acetylene-black concentration.

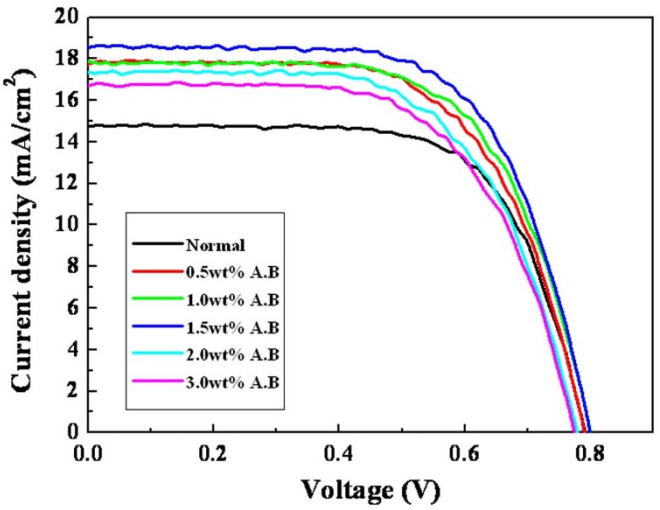

Figure 4 | **J–V curves of the DSSCs fabricated using the Normal films and the TiO_2 photo-electrode films with different concentrations of acetylene-black.**

However, the solar energy-to-electricity conversion efficiency was at its maximum at an acetylene-black concentration of 1.5 wt%, and was decreased above 1.5 wt%. An increase above the critical pore size of TiO_2 photo-electrode films at 1.5 wt% induced a decrease in the relative volume of the TiO_2 photo-anode, resulting in a decrease in the total amount of the adsorbed dye. The efficiency and the short-circuit current density of the DSSC sample with an acetylene-black concentration of 1.5 wt% showed enhancements of about 22 and 26%, respectively, compared with the Normal films DSSC. These results showed that the acetylene-black in the TiO_2 photo-electrode films played an important role in the enhancement of the photo-conversion efficiency of the DSSCs without a light scattering layer.

The internal resistances of the DSSCs were studied via electrochemical impedance spectroscopy (EIS) in the frequency range of 0.1 Hz–100 kHz, and with an alternating current amplitude of 10 mV. Figure 5(a) shows the EIS results at a forward bias of the open-circuit voltage under a light irradiation of 100 mW cm^{-2} with the results represented as Nyquist plots. As shown in Fig. 5(a), three distinct semicircles were observed for the Normal films and TiO_2 films with 1.5 wt% acetylene-black. The impedance plots ordinarily show three semicircles, which were fitted by the equivalent circuit shown in an inset of Fig. 5(a) using the Z-view software. The semicircle at a high frequency was attributed to the counter-electrode charge transfer resistance and Helmholtz capacitance (Rct1 and CPE1) parallel combination (The constant-phase element (CPE1 = $(CPE1\text{-}T)^{-1}(jw)^{-(CPE1-P)}$) was related to the active surface areas of the counter electrode, and the CPE1-P value was related to the porosity of the Pt film). The semicircle observed in the middle frequency was a result of the recombination resistance at the TiO_2/electrolyte interface and the capacitance of the TiO_2 (Rct2 and CPE2). Finally, the third semicircle observed at a low frequency was due to the impedance of diffusion in the electrolyte, the so-called Warburg element (Ws). The widths of the 1, 2 and 3 arcs (at Fig. 5(a)) corresponded to Rct1, Rct2 and R_{Ws}, respectively. The arcs at the high and middle frequency showed similar widths for the Normal films and the 1.5 wt% acetylene-black TiO_2 films, while a clear difference was observed at a low frequency. As shown in Table 1, the average pore size of the TiO_2 photo-electrode films increased as acetylene-black concentrations increased, compared with the Normal films. An increase in the pore size increased the diffusion of the electrolyte into the TiO_2 films, which resulted in a decrease in the R_{Ws}, as shown in Fig. 5(a).

Figure 5(b) shows the incident-photon-to-current-conversion efficiency (IPCE) of the DSSCs of the Normal and TiO_2 films for differing acetylene-black concentrations. The IPCEs were increased with increasing acetylene-black concentration when they were compared with the Normal films, and the IPCE of TiO_2 photo-electrode films with 2.0 wt% acetylene-black is decreased. The increase in IPCEs was consistent with the increase in the J_{SC}, as shown in Fig. 4. The TiO_2 photo-electrode films with 1.5 wt% acetylene-black showed an increase of about 15% compared with that of the Normal films at a peak wavelength of 530 nm. That result indicates that fewer electrons were trapped in the TiO_2 layer because the residual carbons that served as trap densities were reduced by the insertion of the acetylene-black.

Reduction of the trap density by incorporation of the acetylene-black into the TiO_2 anode films was further investigated by the intensity-modulated photovoltage spectroscopy (IMVS). In the present study, IMVS analysis was only investigated because the electron lifetime in the TiO_2 photo-electrode films was closely related to the trap sites such as residual carbons. The IMVS complex plane plots for DSSC cells are shown in Fig. 5 (c) for the Normal films and the TiO_2 photo-electrode films at different acetylene-black concentrations. The DSSC cell comprised of TiO_2 photo-electrode films with 1.5 wt% acetylene-black exhibited the highest photovoltage among the Normal films and the TiO_2 photo-electrode films with the other

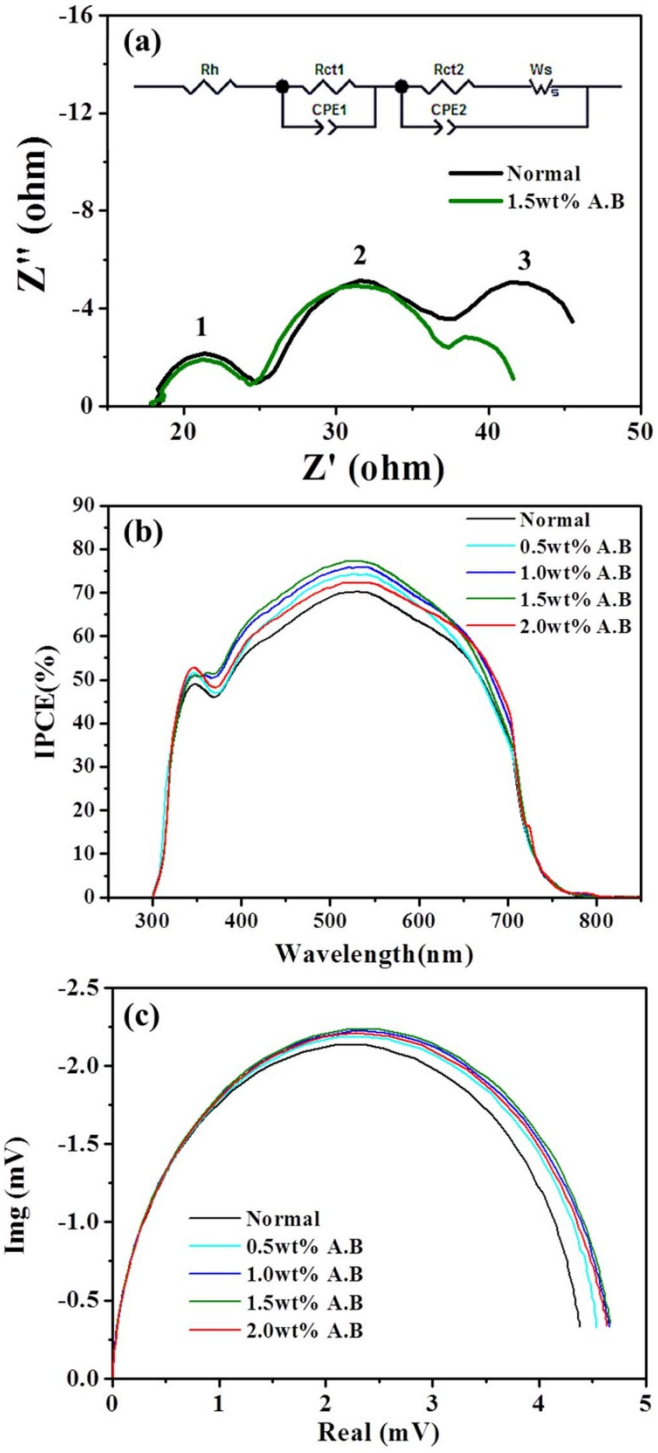

Figure 5 | (a) Nyquist plots of the DSSCs employing the Normal films and 1.5 wt% acetylene-black TiO_2 films. Inset of (a) shows the equivalent circuit. (b) Incident photon to current efficiency (IPCE) of the DSSCs with the Normal films and the TiO_2 photo-electrode films including different acetylene-black concentrations. (c) Intensity-modulated photovoltage spectroscopy (IMVS) presented as polar coordinates in complex plane plots using DSSCs with the Normal films and the TiO_2 photo-electrode films including different acetylene-black concentrations.

acetylene-black concentrations. These results are consistent with those of *J–V* and IPCE. The IMVS is a valuable method for investigating the electron lifetime (τ_r) of photogenerated electrons in TiO_2 photo-electrode films. The electron lifetime can be estimated using

the IMVS plots and the following equation[21,22]:

$$\tau_r = 0.5 \times \pi \times f_{max} \quad (1)$$

where f_{max} is the characteristic frequency at the maximum of the imaginary IMVS. The calculated results are tabulated in Table 3. The increase in the electron lifetimes for TiO_2 photo-electrode films with 0.5 and 1.5 wt% acetylene-black compared with the Normal films is clearly shown in Table 3. On the other hand, the electron lifetimes of the films with 2.0 wt% acetylene-black were decreased, which resulted in similar values for the Normal films. These results were attributed to an increase in the residual carbon quantity. Since the electron recombination takes place via the trap sites at the TiO_2 surface, an insertion of the optimal concentration of acetylene-black removed the trap sites for the generated electrons at the TiO_2 surface.

The qualitative analysis of the residual carbon existing in the Normal films and TiO_2 photo-electrode films with acetylene-black after thermal treatment at 500°C for 30 min was examined using x-ray photoelectron spectroscopy (XPS, MultiLab 2000, Thermo). Those results are valuable in an investigation of the origin of the increases in electron lifetime, IPCE, and J_{sc}. The results are shown in Fig. 6 for the Normal films and the TiO_2 photo-electrode films with different acetylene black concentrations. The surface of samples before measurement was *in situ* etched for 1 min in order to remove the carbon contamination that originated from the ambient air. Small peaks of C 1s emission located at 283.9 eV were detected in all samples. It was apparent that the residual carbons in TiO_2 photo-electrode films were significantly reduced as acetylene black concentrations increased. However, the residual carbons in 2.0 wt% acetylene-black TiO_2 photo-electrode films showed concentrations that were similar to those found in the Normal films because the acetylene-black concentrations were too high to be removed by heat treatment at 500°C for 30 min.

The quantitative analysis of the residual elements existing in the Normal films and TiO_2 photo-electrode films with different acetylene black concentrations was performed using a TruSpec Elemental Analyzer (LECO Co., USA), and the results are summarized for C, H, and N in Table 4. For elemental analysis, samples of about 0.03 g were heated for 1 h at 1050°C for complete combustion. Each C, H, and N decomposed by a complete combustion was collected to analyze the concentration. Compared with the Normal films, samples with an increase in acetylene-black concentration showed a decrease in the residual carbon although the acetylene-black itself includes carbon. The exothermic energy by combustion of the acetylene black contributes for removal of the residual carbon existing already in the Normal films. Therefore, electron lifetime was increased due to a reduction in the trap densities that originated from the residual carbon. A large amount of the dye was adsorbed onto the TiO_2 surface due to less carbon contaminations. In conclusion, an addition of the optimal contents of acetylene-black into the TiO_2 paste played an important role in both the increase of the artificial pores and in the additional removal of the residual carbon in TiO_2 photo- anode films.

In summary, porous anatase-phase TiO_2 nano-crystal (particle size of about 20 nm) films showed a high transparency and had a considerable amount of residual carbon from the organic vehicle of the paste, which resulted in poor light-harvesting efficiency. Acetylene-black paste was applied to meso-porous TiO_2 photo-anodes with a crystalline framework, a low residual carbon, and a tunable pore size. The thermally treated TiO_2 photo-electrode films with increasing acetylene-black concentrations showed an increase in artificial pores and a decrease in the residual carbon compared with the Normal films. The performance of the DSSCs was enhanced using the TiO_2 photo-anode pastes with various acetylene-black concentrations. The photo-conversion efficiency of DSSCs was enhanced from 7.98 (the Normal films) to 9.75% when using TiO_2 photo-electrode films with acetylene-black at 1.5 wt% without a light scattering layer.

Table 3 | Electron lifetime from the IMVS results of DSSC cells prepared using the Normal films and the TiO_2 photo-electrode films with different acetylene-black concentrations

TiO_2 photo-electrode films	Normal	0.5 wt%	1.5 wt%	2.0 wt%
f_{max} (Hz) (Frequency)	0.1711	0.1585	0.1468	0.1711
τ_r (Electron lifetime, s)	0.93	1.00	1.72	0.93

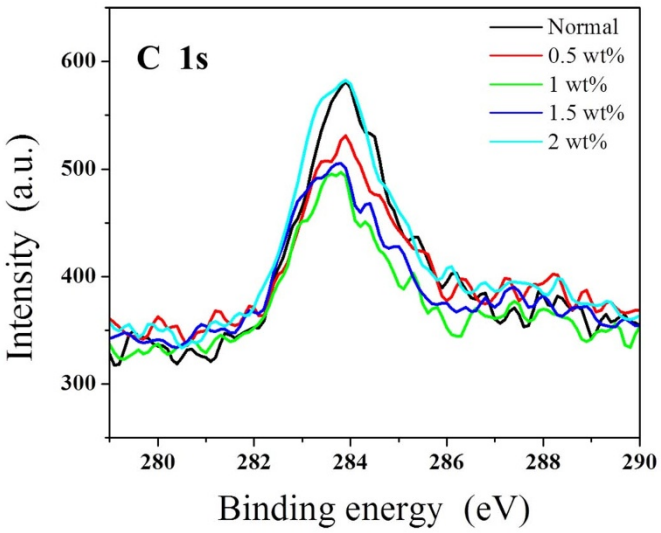

Figure 6 | XPS C 1S spectra of the Normal films and the TiO_2 photo-electrode films with different acetylene-black concentrations treated at 500°C for 30 min.

Methods

Preparation of acetylene-black TiO_2 paste. For the formation of artificial pores in the TiO_2 photo-electrode films, acetylene-black TiO_2 pastes were prepared using a paste-blending method. First, a TiO_2 colloidal solution was synthesized by the hydrothermal growth method shown in Figure S1 (Supporting Information), and it was used for the starting material. Acetylene-black powder was purchased from the Chevron Phillips Chemical Company. Figure S2 (Supporting Information) shows a schematic diagram of the combustion process for the synthesis of the TiO_2 paste with acetylene-black. Acetylene-black TiO_2 paste was prepared by the addition of ethylene carbonate for the binder and terpineol for the solvent of a TiO_2 colloidal solution (particle size of about 20 nm), followed by a mixing process using a paste blender. Then, acetylene- black powder was added and the paste was continuously mixed. After that, mixed paste was dried at 80°C for 2 h using a rotary evaporator to obtain a screen printable viscosity. Various concentrations (0.5, 1.0, 1.5, 2.0, and 3.0 wt%) of acetylene-black powders were used to prepare the optimal acetylene-black paste. The TiO_2 photo-anode paste with various acetylene-black concentrations was characterized using TG/DTA equipment. In order to investigate the thermal decomposition of the acetylene-black in a real DSSC device, TG/DTA analysis was performed using the TiO_2 powders including the 1.5 wt% acetylene-black treatment at each temperature for 30 min.

Preparation of the TiO_2 photo-electrode films. TiO_2 pastes with and without acetylene-black for TiO_2 photo-electrode films were deposited onto the conducting glass of a fluorine-doped stannic oxide layer (FTO, TEC 8/2.3 mm, 8 Ω/□,

Table 4 | Elemental concentration existing in the Normal films and the TiO_2 photo-electrode films with different acetylene-black concentrations

TiO_2 photo-electrode films	Elemental Composition (wt%)		
	Carbon (C)	Hydrogen (H)	Nitrogen (N)
Normal	0.16	1.27	N.D
0.5 wt% A.B	0.13	1.01	N.D
1.0 wt% A.B	0.11	1.32	N.D

Pilkington) using a screen-printing method. The resultant layer was treated for 30 min at 500°C in ambient air using a muffle furnace. The screen printing and the thermal treatment process was repeated until a thickness of about 14 μm was obtained. The area of the prepared porous TiO_2 electrode was about 5×5 mm^2. Dye adsorption was carried out by dipping the TiO_2 electrode films into a 4×10^{-4} M t-butanol/acetonitrile (Merck, 1 : 1) solution of the standard ruthenium dye (N719 (Solaronix)) for 48 h at 25°C. The morphologies and quantitative compositions of the residual elements of the Normal films and TiO_2 photo-electrodes with acetylene-black after thermal treatment at 500°C for 30 min were investigated using SEM and a TruSpec Elemental Analyzer (LECO Co., USA), respectively. Absorption of dye-adsorbed TiO_2 films was characterized using a UV-vis spectrophotometer (S-3100, SCINCO, Co.). The quantitative analysis of the dye adsorbed into the Normal films and TiO_2 photo-electrode films with 1.5 wt% acetylene-black was performed using a UV-vis-NIR spectrometer (UV-vis-NIR Agilent, USA).

Fabrication of the DSSCs. The fabrication process for the DSSCs is schematically shown in Figure S3 (Supporting Information). Transparent counter electrodes were prepared by placing a few drops of 10 mM hydrogen hexachloroplatinate (IV) hydrate (99.9%, Aldrich) into a 2-propanol solution on drilled FTO glass plates (TEC 8/2.3 mm, 8 Ω/□, Pilkington). After treatment at 400°C for 30 min, the counter electrode was assembled with the TiO_2 electrode. The two electrodes were separated using 60 μm of Surlyn, and were then sealed by heating. The internal space was filled with the electrolyte through the drilled hole, which was then sealed with Surlyn and a cover-glass. The IMVS was measured using a ZAHNER Potentiostat with the same sandwich-cell setup. A light emitting diode (LED, 635 nm) was used as the light source. The light intensity was modulated with sine-shaped voltage supplied by a Solartron 1255B frequency response analyzer (FRA) over an appropriate frequency range of from 10 mHz to 100 Hz. The light intensity in the present study was maintained at 10 W m^{-2}.

Photovoltaic characterization of the DSSCs. The photovoltaic properties of the prepared DSSCs were measured using a computer-controlled digital source meter (potentiostat/galvanostat Model 273A, EG&G) and a solar simulator (AM 1.5, 100 mW cm^{-2}, Oriel) as a light source. The light intensity was adjusted with a reference Si cell (Fraunhofer Institute for Solar Energy System). Photovoltaic performance was characterized by V_{oc}, J_{sc}, and *FF* (fill factor), and the overall efficiency was characterized using the current density-voltage (*J–V*) curve.

1. Wongcharee, K., Meeyoo, V. & Chavadej, S. Dye-sensitized solar cell using natural dyes extracted from rosella and blue pea flowers. *Sol. Energ. Mat. Sol. C.* **91**, 566–571 (2007).
2. Hao, S., Wu, J., Huang, Y. & Lin, J. Natural dyes as photosensitizers for dye-sensitized solar cell. *Sol. Energy* **80**, 209–214 (2006).
3. Polo, A. S. & MurakamiIha, N. Y. Blue sensitizers for solar cells: Natural dyes from Calafate and Jaboticaba. *Sol. Energ. Mat. Sol. C.* **90**, 1936–1944 (2006).
4. Nazeeruddin, M. K. *et al.* Conversion of light to electricity by cis-X2bis(2,2'-bipyridyl-4,4'-dicarboxylate)ruthenium(II) charge-transfer sensitizers (X = Cl-, Br-, I-, CN-, and SCN-) on nanocrystalline titanium dioxide electrodes. *J. Am. Chem. Soc.* **115**, 6382–6390 (1993).
5. Chiba, Y., Islam, A., Komiya, R., Koide, N. & Han, L. Conversion efficiency of 10.8% by a dye-sensitized solar cell using a TiO_2 electrode with high haze. *Appl. Phys. Lett.* **88**, 223505-1-3 (2006).
6. Koo, H. J. *et al.* Nano-embossed Hollow Spherical TiO_2 as Bifunctional Material for High-Efficiency Dye-Sensitized Solar Cells. *Adv. Mater.* **20**, 195–199 (2008).
7. Ni, M., Leung, M. K. H., Leung, D. Y. C. & Sumathy, K. Theoretical modeling of TiO_2/TCO interfacial effect on dye-sensitized solar cell performance. *Sol. Energ. Mat. Sol. C.* **90**, 2000–2009 (2006).
8. O'Regan, B. & Grätzel, M. A low-cost, high-efficiency solar cell based on dye-sensitized colloidal TiO_2 films. *Nature* **353**, 737–740 (1991).
9. Wang, P., Zakeeruddin, S. M., Exnar, I. & Grätzel, M. High efficiency dye-sensitized nanocrystalline solar cells based on ionic liquid polymer gel electrolyte. *Chem. Commun.* **24**, 2972–2973 (2002).
10. Nazeeruddin, M. K. *et al.* Engineering of Efficient Panchromatic Sensitizers for Nanocrystalline TiO_2-Based Solar Cells. *J. Am. Chem. Soc.* **123**, 1613–1624 (2001).
11. Yang, C. C., Zhang, H. Q. & Zheng, Y. R. DSSC with a novel Pt counter electrodes using pulsed electroplating techniques. *Curr. Appl. Phys.* **11**, S147–S153 (2011).
12. Nelson, K. & Deng, Y. Effect of polycrystalline structure of TiO_2 particles on the light scattering efficiency. *J. Colloid Interf. Sci.* **319**, 130–139 (2008).
13. Hore, S., Vetter, C., Kern, R., Smit, H. & Hinsch, A. Influence of scattering layers on efficiency of dye-sensitized solar cells. *Sol. Energ. Mat. Sol. C.* **90**, 1176–1188 (2006).
14. Yang, L. *et al.* Light harvesting enhancement for dye-sensitized solar cells by novel anode containing cauliflower-like TiO_2 spheres. *J. Power Sources* **182**, 370–376 (2008).
15. Zhao, X., Lin, H., Li, X. & Li, J. The application of freestanding titanate-nanofiber paper for scattering layers in dye-sensitized solar cells. *Mater. Lett.* **65**, 1157–1160 (2011).
16. Chuangchote, S., Sagawa, T. & Yoshikawa, S. Efficient dye-sensitized solar cells using electrospunTiO_2 nanofibers as a light harvesting layer. *Appl. Phys. Lett.* **93**, 033310-1-3 (2008).
17. Kang, S. H. *et al.* Influence of light scattering particles in the TiO_2 photoelectrode for solid-state dye-sensitized solar cell. *J. Photoch. Photobio. A Chem.* **200**, 294–300 (2008).
18. Ferber, J. & Luther, J. Computer simulations of light scattering and absorption in dye-sensitized solar cells. *Sol. Energ. Mat. Sol. C.* **54**, 265–275 (1998).
19. Rothenberger, G., Comte, P. & Grätzel, M. A contribution to the optical design of dye-sensitized nanocrystalline solar cells. *Sol. Energ. Mat. Sol. C.* **58**, 321–336 (1999).
20. Lee, B. K. & Kim, J. J. Enhanced efficiency of dye-sensitized solar cells by UV-O_3 treatment of TiO_2 layer. *Curr. Appl. Phys.* **9**, 404–408 (2009).
21. Lee, B. H. *et al.* Charge transport characteristics of high efficiency dye-sensitized solar cells based on electrospun TiO_2 nanorod photoelectrodes. *J. Phys. Chem. C* **113**, 21453–21457 (2009).
22. Archana, P. S., Jose, T., Vijila, C. & Ramakrishna, S. Improved electron diffusion coefficient in electrospun TiO_2 nanowires. *J. Phys. Chem. C* **113**, 21538–21542 (2009).

Acknowledgements

This work was supported by a National Research Foundation of Korea (NRL) grant funded by the Korea Government (MEST) (No. 2011-0000359). This work was supported by the International Collaborative R&D Program of the Korea Institute of Energy Technology Evaluation and Planning (KETEP) grant funded by Korea government Ministry of Knowledge Economy [20118520010020]. Authors thank Prof. Young-Seak Lee for valuable discussion of EIS analysis.

Author contributions

All authors reviewed the manuscript. T. Y. and C. H. designed experiments, performed research, and analyzed the data. Y. J. designed experiments. S. G. designed experiments, analyzed the data, and wrote the paper.

Additional information

Supplementary information accompanies this paper at http://www.nature.com/scientificreports

Competing financial interests: The authors declare no competing financial interests.

How to cite this article: Cho, T.-Y., Han, C.-W., Jun, Y.S. & Yoon, S.-G. Formation of artificial pores in nano-TiO_2 photo-electrode films using acetylene-black for high-efficiency, dye-sensitized solar cells. *Sci. Rep.* **3**, 1496; DOI:10.1038/srep01496 (2013).